Astrophysics and Space Science
DOI 10.1007/s●●●●●-●●●-●●●●-●

Stellar winds from hot low-mass stars

W.-R. Hamann[1]

Abstract Stellar winds appear as a persistent feature of hot stars, irrespective of their wide range of different luminosities, masses, and chemical composition. Among the massive stars, the Wolf-Rayet types show considerably stronger mass loss than the O stars. Among hot low-mass stars, stellar winds are seen at central stars of planetary nebulae, where again the hydrogen-deficient stars show much stronger winds than those central stars with "normal" composition. We also studied mass-loss from a few extreme helium stars and sdOs. Their mass-loss rate roughly follows the same proportionality with luminosity to the power 1.5 as the massive O stars. This relation roughly marks a lower limit for the mass loss from hot stars of all kinds, and provides evidence that radiation pressure on spectral lines is the basic mechanism at work. For certain classes of stars the mass-loss rates lie significantly above this relation, for reasons that are not yet fully understood. Mass-loss from low-mass stars may affect their evolution, by reducing the envelope mass, and can easily prevent diffusion from establishing atmospheric abundance patterns. In close binary systems, their winds can feed the accretion onto a companion.

Keywords Stellar winds – mass loss

1 Introduction: winds from hot stars

Hot stars of various types lose mass through stellar winds (see Fig. 1). Massive stars lose mass as O or B-type stars (OB), Luminous Blue Variables (LBV), or Wolf-Rayet (WR) stars, before they finally explode as supernova. Among low-mass stars, central stars of planetary nebulae (CSPNe) show stellar winds. They are on the track from the Asymptotic Giant Branch (AGB) to the white dwarf cooling sequence. Extreme helium (EHe) stars and subdwarf-O (sdO) stars are further types of low-mass stars which are found to display signs of mass-loss. Their evolutionary origin is attributed to binarity (Saio and Jeffery 2002; Heber 2009).

Prototype for an O-type star with mass loss is the O5 supergiant ζ Puppis. Striking evidence for the stellar wind comes from the P-Cygni profiles of resonance lines in the UV (cf. Fig. 2, left panel). However, these profiles are often saturated and therefore not sensitive for a precise determination of the mass-loss rates. The optical spectrum shows mostly "normal" absorption lines, while Hα is in emission (cf. Fig. 2, right panel). Mass-

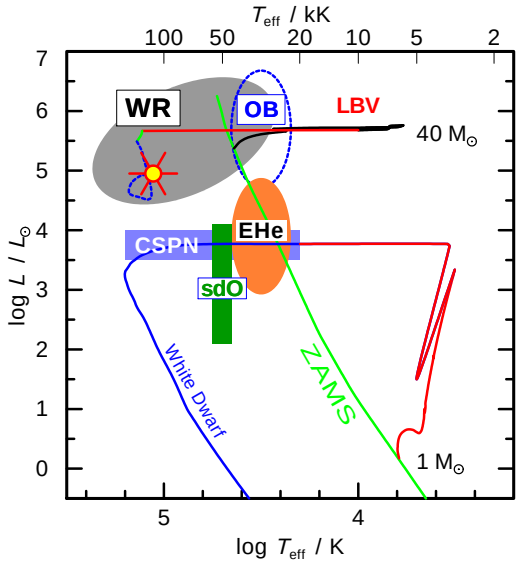

Fig. 1 Location of various types of hot stars (see text) with mass loss in the Hertzsprung-Russell-Diagram (HRD). The Zero Age Main Sequence (ZAMS) is indicated together with evolutionary tracks for a massive (40 $M_\odot$) star and a low-mass (1 $M_\odot$) star.

W.-R. Hamann
[1]Institut für Physik und Astronomie, Universität Potsdam, Germany

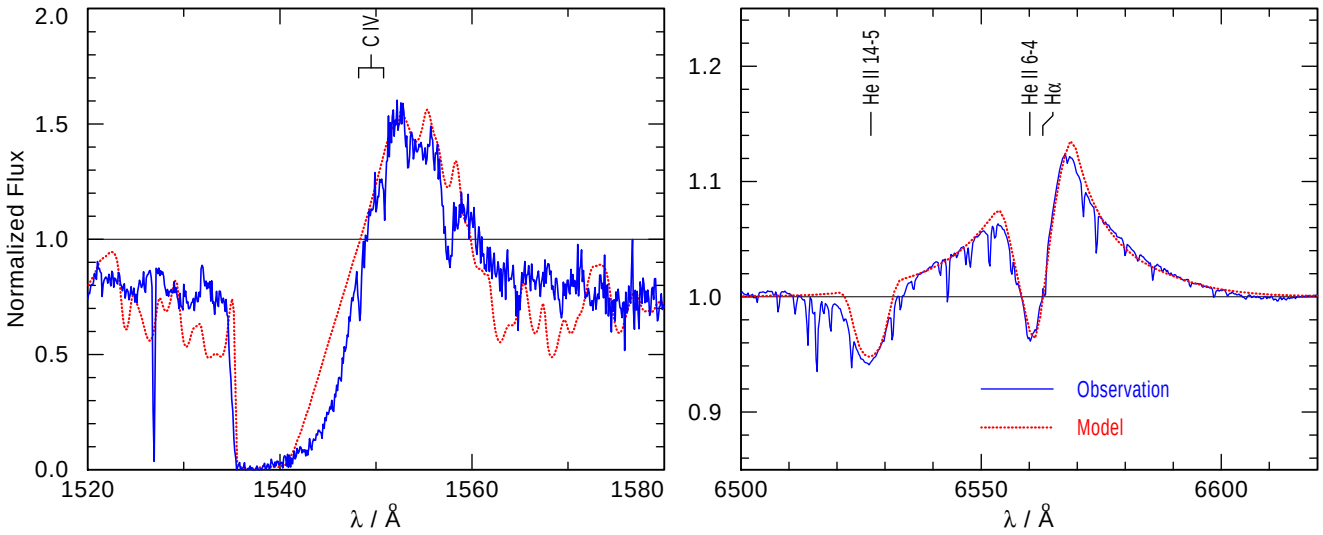

Fig. 2 Observed spectrum (blue) of ζ Puppis around the C IV resonance doublet (left frame) and Hα (right frame), and a model fit (red-dotted) calculated with the Potsdam Wolf-Rayet (PoWR) model atmosphere code.

loss rates from O stars are most conveniently determined from fitting this line with model calculations. However, as the Hα emission is powered from the recombination cascade, it depends on the degree of small-scale inhomogeneity which is poorly known (Hamann, Feldmeier, and Oskinova 2008). Empirical mass-loss rates decrease when "micro-clumping" is taken into account. Mass-loss rates derived from (preferably unsaturated) UV resonance lines do not suffer from this problem since their opacity depends linearly on density. However, it was shown by Oskinova, Hamann, and Feldmeier (2007) that inhomogeneities on larger scale ("macroclumping") can affect these lines, this time leading to under-estimating the mass-loss rates.

Hot star winds are driven by the radiation field. Stellar radiation is intercepted by spectral lines, where the photons deliver their momentum $h\nu/c$. As the wind accelerates to the terminal wind velocity v_∞, the spectral line becomes Doppler-shifted and sweeps up the radiation over the whole frequency band $\Delta\nu = \nu_0\ v_\infty/c$. Hence the momentum that is intercepted by one optically thick line per time is $L_{\nu_0}\ \Delta\nu/c$, which is of the order of $L\ v_\infty/c^2$ for a line frequency at about the flux maximum (cf. Fig. 3). This intercepted momentum rate can be compared with the mechanical momentum carried by the wind per time, $\dot{M}\ v_\infty$. Thus, one optically thick line drives a mass-loss of $\dot{M} = L/c^2$ – interestingly the same rate by which the star must convert mass into energy to sustain its luminosity L.

In a seminal paper, Castor, Abbott, and Klein (1975) have shown that for a mixture of optically thick and thin lines the hydrodynamic equation has a stationary solution with the mass-loss rate $\dot{M}$ as its eigenvalue. After some minor modifications, this theory can well explain the observed mass loss from OB stars like, e.g., ζ Puppis.

The highest mass-loss rate that can be achieved by the Castor, Abbott, and Klein (1975) theory is obviously reached when the momentum from all photons is transferred to the wind, i.e. $\dot{M}\ v_\infty = L/c$. The winds of Wolf-Rayet stars, however, are often even stronger and exceed this so-called single-scattering limit. In order to drive the strong WR winds, multiple scattering must be taken into account. Adequate hydrodynamical models for WR stars have been successfully computed (Gräfener and Hamann 2005, 2008), thus demonstrating that WR winds can also be radiation-driven.

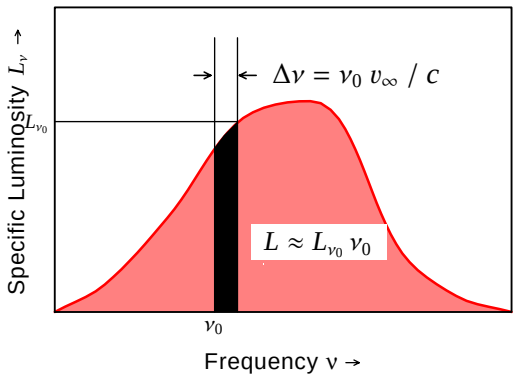

Fig. 3 Line driving of a stellar wind. Due to the Doppler shift, one single optically thick line sweeps up all radiation within the frequency interval $\Delta\nu$. When the line frequency ν_0 is located at about the flux maximum, the specific luminosity L_{ν_0} is of the order of L/ν_0. This allows to estimate the mass-loss driven by one single line (see text).

2 Mass loss from hot stars

2.1 Model atmospheres

Mass-loss becomes manifest in the stellar spectrum. Thin winds may only affect a few UV resonance lines that become asymmetrically broadened; in stronger winds, these broadened, blue-shifted absorptions are accompanied by a red-shifted emission feature (P-Cygni profile), while in very dense winds the whole line spectrum may appear in emission (Wolf-Rayet types). In order to determine the mass-loss rates, adequate models must be compared to the observation. Such models are provided by the Potsdam Wolf-Rayet (PoWR) model atmosphere code (Hamann and Gräfener 2004, and references therein).

This code solves the non-LTE radiative transfer in a spherically symmetric expanding atmosphere. Mass-loss rate and wind velocity are free parameters of the models. Wind inhomogeneities ("clumping") are accounted for in a first-order approximation, assuming that optically thin clumps fill a volume fraction $f_{\rm V}$ while the interclump space is void. Thus the matter density in the clumps is higher by a factor $D = f_{\rm V}^{-1}$, compared to an un-clumped model with the same parameters. The proper values for this clumping contrast is highly debated (see Hamann, Feldmeier, and Oskinova 2008).

Detailed model atoms of the most relevant elements (H, He, C, N, O, Si) are taken into account in our models. Typically, 400 non-LTE levels and 5000 line transitions are explicitely treated. Additionally, about 10^5 energy levels and 10^7 line transitions of iron and other iron-group elements are approximately included using the "superlevel" approach. In addition to Doppler broadening from thermal motion and microturbulence, radiation damping and pressure broadening are accounted for in the formal integral. These new extensions of the PoWR code are especially important for studying stars with thin winds, where most of the spectral lines are formed in the photosphere.

As already mentioned, the velocity field must be prespecified. In the subsonic region, $v(r)$ is defined such that a hydrostatic density stratification is approached. For the supersonic part we adopt the usual β-law, basically of the form $v(r) = v_\infty(1-1/r)^\beta$, with the terminal velocity v_∞ being a free parameter. The exponent β is chosen between 0.7 and 1.0 such that the wind profiles are reproduced best. If appropriate, we sometimes employ a "double beta law", which means that a second term of the same β-law form is added to the velocity, but with a larger value for the exponent (e.g. $\beta = 4$).

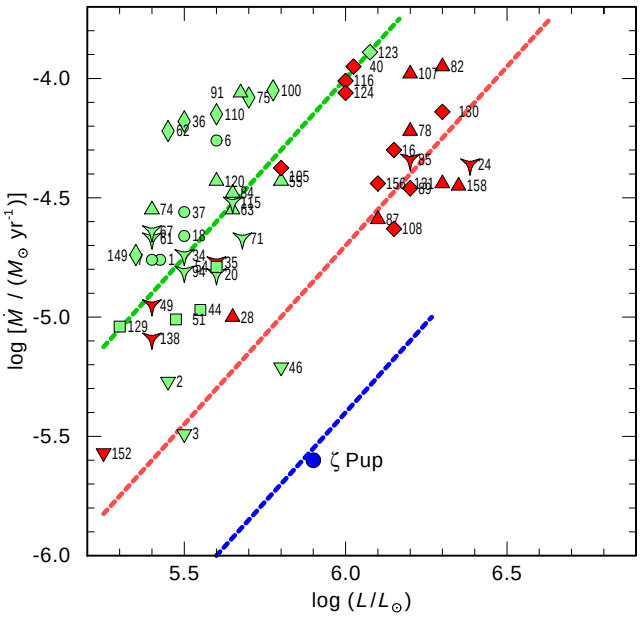

Fig. 4 Mass-loss rates versus luminosity for massive stars. O-stars are represented by the prototype ζ Puppis, while the values for other O stars roughly follow the blue-dashed line. The other points refer to Wolf-Rayet stars (labelled by their WR catalog numbers), where the red (dark) filled symbols are "late" WN subtypes and the green (light) symbols represent "early" subtypes. The dashed lines are tentative fits with the same slope 1.5 for either groups.

2.2 Massive stars

Empirical mass-loss rates have been determined for a multitude of O-stars. In Fig. 4 they are represented by the prototype ζ Puppis, while the values for other O stars roughly follow the (blue) dashed line with the slope $\log \dot{M} \propto 1.5 \log L$. The Galactic Wolf-Rayet stars of the nitrogen sequence (i.e. WN types) have comprehensively analyzed by Hamann, Gräfener, and Liermann (2006). The "late" WN subtypes (WNL), which are characterized by an atmospheric composition that still contains some hydrogen, have mass-loss rates that are roughly five times higher than for O stars of same luminosity, as tentatively indicated by the middle dashed (red) line in Fig. 4. The hydrogen-free "early" WN subtypes (WNE) have smaller luminosities, but similarly high mass loss as the WNL, and thus their tentative $\dot{M}$-L relation lies another factor five higher. – For Wolf-Rayet stars of the carbon sequence (WC), a comprehensive analysis is still needed.

2.3 Central stars of planetary nebulae

The determination of mass-loss rates for Galactic CSPNe suffers from the uncertainty of their distance. The vast majority of CSPNe show a "normal",

hydrogen-rich atmospheric composition and thus an O-star spectrum. Figure 5 includes nine O-type CSPNe analyzed by Kudritzki, Urbaneja, and Puls (2006) with current model atmospheres (full blue circles). In their semi-empirical approach, the mass-loss rate is a free parameter, and the distance is obtained "spectroscopically" via $T_{\rm eff}$, $\log g$ and the mass-luminosity relation for post-AGB stars.

Pauldrach, Hoffmann, and Méndez (2004) analyzed the same sample of stars, but rather relied on their hydrodynamical models than on the mass-luminosity relation from evolutionary tracks (Fig. 5, open blue circles). Apart from the apparent inconsistency, both approaches lead to relatively high luminosities above $10^4 L_\odot$ for most of the stars. This challenges the traditional opinion dating back to e.g. Schoenberner (1983) that typical CSPNe evolve at $5000\,L_\odot$ and become white dwarfs with $0.6\,M_\odot$. According to these studies, the [O]-type CSPNe show amazingly high mass-loss rates.

For a few planetary nebulae the distance can be determined from the expansion parallax. Based on such distance, Georgiev *et al.* (2008) obtained a contrastingly *low* luminosity for the O-type central star of the Cat's Eye nebula (NGC 6543), also shown in Fig. 5. Albeit a correct application of this method needs sophisticated modeling of the nebular evolution (see Schönberner, Jacob, and Steffen 2005), it could be exploited for a few more CSPNs with winds.

Taking advantage of the known distance, Herald and Bianchi (2004) analyzed CSPNe in the Large Magellanic Cloud (LMC). The five hydrogen-rich CSPNe from their sample are also included in Fig. 5 (blue triangles). In puzzling contrast to the Galactic studies quoted above, their CSPN luminosities never exceed the canonical value of $\log L/L_\odot = 3.7$, some of them even being much fainter. The mass-loss rates (adopting a clumping contrast of D=10) are by one order of magnitude smaller than found for the Galactic sample.

CSPNe with hydrogen-deficient atmospheres usually show a Wolf-Rayet type spectrum as evidence for strong mass loss. According to their effective temperature, they are divided into two clearly distinct classes, the early [WCE] and the late [WCL] subtypes. A sample of eleven Galactic [WCE] stars has been recently analyzed by Todt *et al.* (in preparation) with PoWR models. For the luminosity the canonical value of $\log L/L_\odot = 3.7$ has been adopted (squares with red/dark filling in Fig. 5). Exploiting its known distance, the [WCE] central star of LMC-SMP61 in the Large Magellanic Cloud has been analyzed by (Stasińska *et al.* 2004) with the results plotted in Fig. 5. Slightly different parameters for this star were obtained by Herald and Bianchi (2004).

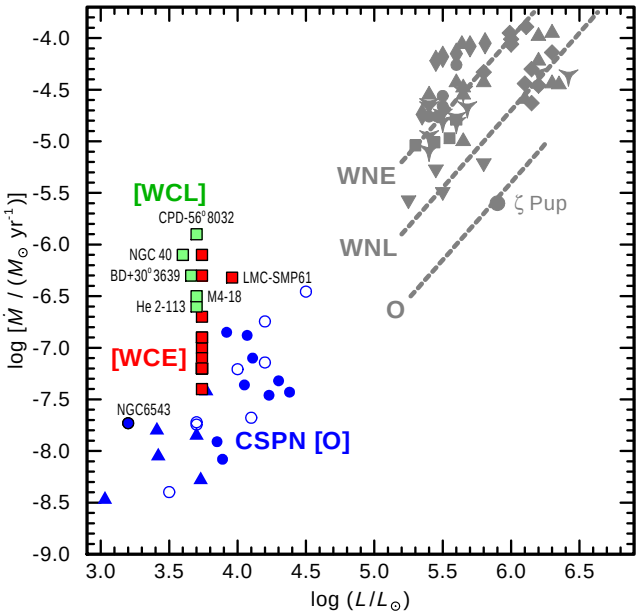

Fig. 5 Mass-loss rates versus luminosity for Central Stars of Planetary Nebulae. Blue, unlabeled circles are for a sample of nine O-type central stars with hydrogen-rich composition. Wolf-Rayet type central stars are indicated by squares. Red/dark filling stands for "early" subtypes, [WCE], while the green/light filled squares with labels are "late" subtypes, [WCL]. Massive stars are included for comparison (grey).

From various sources we collect a few Galactic late-type Wolf-Rayet central stars ([WCL]) for which independent distance estimates exist (squares with green/light filling in Fig. 5). Most significant is the analysis of BD+30°3639, which has an expansion parallax, by Marcolino *et al.* (2007).

Inspecting Fig. 5 with respect to the CSPN mass-loss rates, the lowest values are found for the hydrogen-rich [O]-type central stars (especially when disregarding the spurious results for the Galactic [O]-type CSPN). For the Wolf-Rayet type central stars, $\dot{M}$ is much higher, about ten times for the early subtypes ([WCE]) and up to 100 times for the late ([WCL]).

2.4 Extreme helium stars

Amongst the hot stars in the Galaxy is a collection of low-mass but nevertheless luminous stars from whose surfaces hydrogen is almost completely absent. Instead they are composed principally of helium and some 3% carbon (by mass). The hottest of these "extreme helium stars" are helium-sdOs. Increasing evidence has accrued that these stars are the result of a merger between a helium- and a carbon/oxygen white dwarf. In such stars the helium white dwarf is entirely disrupted, wrapping itself around its more massive companion,

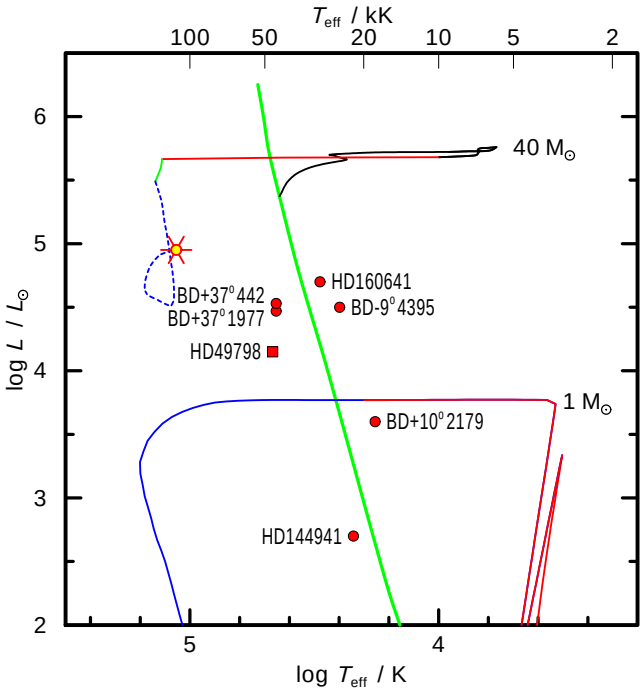

Fig. 6 HRD showing the six extreme helium stars (dots) and the sdO star HD 49798 (square) for which the mass-loss is being discused in this paper.

whereupon a helium shell is ignited and the star becomes a helium supergiant for a few tens of thousands of years, before contracting to become a massive C/O white dwarf (e.g. Saio and Jeffery 2002).

In a recent paper (Jeffery and Hamann 2010) we have analyzed six such extreme helium stars with respect to their mass loss. Their location in the HRD is shown in Fig. 6. Since the winds from these stars are weak, their spectra mainly form in the nearly hydrostatic photosphere. Only the strongest UV resonance lines are contaminated by the stellar wind.

All our program stars have been previously studied with static models, yielding the effective temperature $T_{\rm eff}$, the surface gravity $\log g$, the stellar luminosity L, and the chemical composition. Spectroscopic masses, distances and luminosities are derived via the core mass

Table 1 Parameters of extreme helium stars

Star	$T_{\rm eff}$ [kK]	$\log L$ [$L_\odot$]	v_∞ [km/s]	$\log \dot{M}$ [$M_\odot$/yr]
BD+37°1977	48.0	4.4	2000	−8.2
BD+37°442	48.0	4.4	2000	−8.5
HD160641	35.5	4.5	500	−7.3
BD−9°4395	25.1	4.4	400	−7.9
BD+10°2179	18.5	3.6	400	−8.9
HD144941	27.0	2.7	500	−9.8

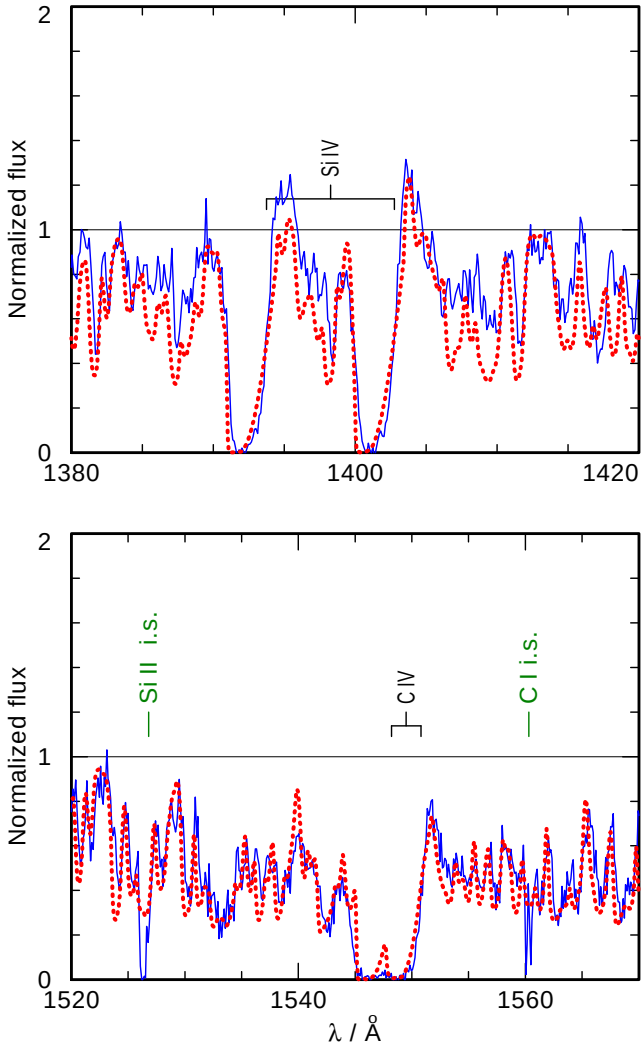

Fig. 7 Normalized spectrum of the extreme helium star HD 160641 (alias V2076 Oph) with the UV resonance doublets of Si IV (top) and C IV (bottom). The numerous other features belong to the "forest" of iron lines. Observations are in blue, while the model calculation is red-dotted.

– luminosity relation for He-shell burning stars (Jeffery 1988). In the recent paper we first checked the fit of the photospheric spectrum and revised the parameters if necessary. Then the stellar-wind parameters, essentially the mass-loss rate $\dot{M}$ and the terminal wind velocity v_∞, are fine-tuned in order to reproduce the profiles of the wind-contaminated UV resonance lines. An example is shown in Fig. 7. The final parameters of the whole sample are compiled in Table 1.

It has been theoretically predicted that in very thin winds the radiation pressure will accelerate only the metal ions, while the bulk matter of hydrogen or helium stays inert. This *ion decoupling* would lead to frictional heating, or perhaps even to instabilities that completely disrupt the smooth stellar wind (Springmann and Paul-

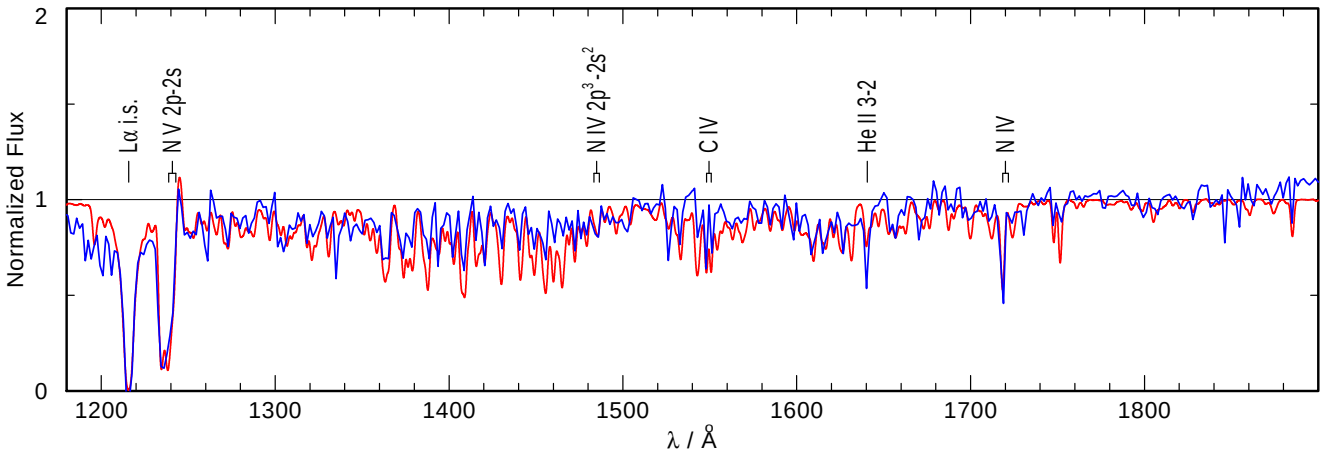

Fig. 8 The UV spectrum of the sdO star HD 49798. The IUE observation (blue continuous line) is compared to a PoWR model (red dotted line) with the parameters as given in the text.

drach 1992; Krtička and Kubát 2001). Among our program stars, the thinnest wind is encountered at the extreme helium star BD+10°2179. According to our fit model, the number density at one stellar radius from the photosphere is about $10^{8.0}$ atoms per cubic centimeter. Mass-loss rate and radius of that star are almost identical to those of τ Sco, for which ion decoupling has been predicted. Indeed, we found that the C IV resonance line observed in the spectrum of BD+10°2179 cannot be explained by models in radiative equilibrium, and therefore speculated that this "superionization" is caused by frictional heating from ion decoupling (Jeffery and Hamann 2010).

Another mechanism that can cause superionization is by X-rays. Radiation-driven winds are known to produce X-rays, probably in wind-embedded shocks (e.g. Oskinova, Feldmeier, and Hamann 2006). While in dense winds the X-ray photons have little influence on the bulk of the "cool" wind matter, they may compete better with the recombination rates in very thin winds. Unfortunately, our hot low-mass stars are too faint to be detectable in X-rays.

2.5 Mass loss from sdO stars

Four subdwarf-O stars had been examined for indications of stellar winds in our early paper Hamann *et al.* (1981). HD 127493 did not show any wind signatures in its UV spectrum, and BD+75°325 exhibited only a marginal line asymmetry. HD 128220B presents the N V resonance doublet as weak P-Cygni profile, while in the spectrum of HD 49798 the nearly saturated P-Cygni profile of this line indicates a relatively strong mass loss of $\log \dot{M}/(M_\odot\,\mathrm{yr}^{-1}) = -9.3 \ldots -8.0$. However, this rate was estimated on the basis of two-level-atom modeling

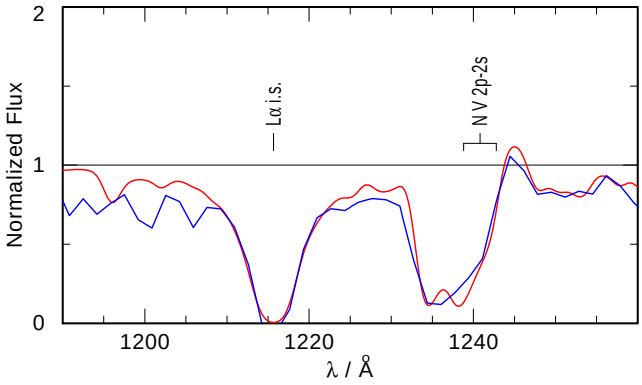

Fig. 9 Same as Fig. 8, now zooming at the N V resonance doublet which indicates the stellar wind.

without a consistent calculation of the ionization structure.

Therefore we found it worth to revisit HD 49798. This star is an X-ray binary, where a white dwarf accretes matter from the wind of the sdO component. Mereghetti *et al.* (2009) could use the time-delay of the pulsed X-rays to fully determine the binary parameters, and found that the white dwarf is unusually massive ($> 1.2\,M_\odot$) and thus close to the Chandrasekhar limit. The photospheric spectrum of the primary, i.e. the sdO star, has been re-analyzed recently by Przybilla *et al.* (these proceedings). We adopt their $T_{\rm eff} = 46.5$ kK, $\log g = 4.35$, and abundances H:He = 20:80 (by mass). Further abundances are set to $X_{\rm C} = 10^{-4}$, $X_{\rm N} = 0.01$, and $X_{\rm Fe} = 0.0011$.

Our PoWR model perfectly fits the spectral energy distribution from the UV to the 2MASS photometry, when we set the distance according to the mean value of the HIPPARCOS parallax ($\pi = 1.2 \pm 0.5$ mas) while adjusting the reddening to $E_{\rm B-V} = 0.06$ mag and the

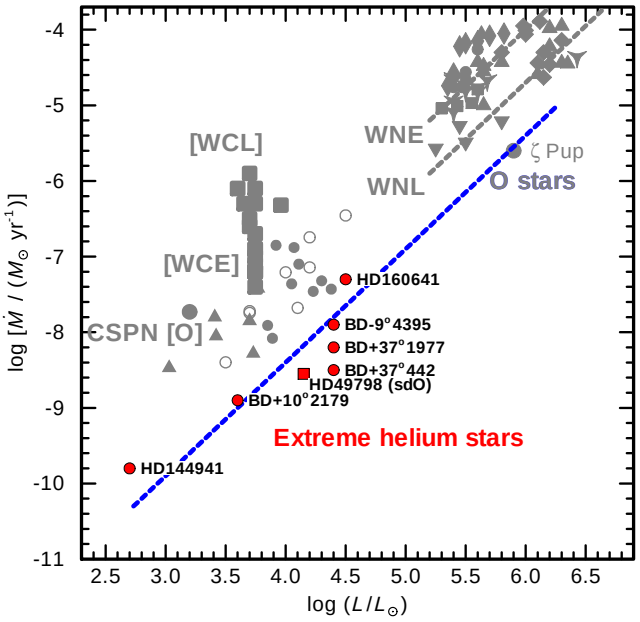

Fig. 10 Mass-loss rate versus luminosity for the various types of hot stars of high and low masses. The labelled red dots represent extreme helium stars, the red square the O-subdwarf HD49798. Grey groups of symbols denote central stars of planetary nebulae of hydrogen-rich composition (CSPN [O], dots) or of Wolf-Rayet type (squares: [WCE], diamonds: [WCL]), see Fig. 5 for more details. Also in grey are the massive Wolf-Rayet stars (squares: WNE, diamonds: WNL, cf. Fig. 4). The long blue dashed line gives the relation $\dot{M} \propto L^{1.5}$, tied to the prototype O-type supergiant ζ Puppis.

luminosity to $\log L/L_\odot = 4.15$. This model also reproduces the UV spectrum with the iron-line forest (Fig. 8). A zoom into the N V resonance doublet is shown in Fig. 9. The terminal wind velocity of $v_\infty = 1350\,\mathrm{km/s}$ from Hamann *et al.* (1981) is confirmed, and the mass-loss rate is adjusted to $\log \dot{M}/(M_\odot\,\mathrm{yr}^{-1}) = -8.55$, somewhere in the middle of the wide range given in the old paper.

3 Conclusions

As a general result, stellar winds appear as a persistent feature of hot stars, irrespective of their wide range of different luminosities, masses and chemical composition. In Fig. 10 we plot the empirical mass-loss rates $\dot{M}$ versus the stellar luminosity L, both on logarithmic scale. The theory of radiation-driven winds in its most elementary form (Castor, Abbott, and Klein 1975) predicts a correlation of about $\dot{M} \propto L^{1.5}$, which in first approximation also holds for the later refinements of this prediction like the "modified wind momentum – luminosity relationship" (see e.g. Puls, Vink, and Najarro 2008). Fig. 10 reveals that this relation, represented by the long blue dashed line normalized to the values for the massive O-type supergiant ζ Puppis, marks indeed a rough lower limit for the mass loss from hot stars of all kinds.

Among the massive stars, the Wolf-Rayet types show considerably stronger mass loss than the O stars. Mass-loss rates of similarly height ($\log \dot{M}/(M_\odot\,\mathrm{yr}^{-1}) = -5$ ... -4) are found for the early subtypes (WNE) as well as for the late subtypes (WNL), albeit the latter typically have higher luminosities. According to detailed hydrodynamic modelling, the extremely strong mass loss from Wolf-Rayet stars is caused by their proximity to the Eddington limit, and driven by multiple line scattering (Gräfener and Hamann 2008).

Among hot low-mass stars, stellar winds are especially observed at central stars of planetary nebulae (CSPN). In their majority the CSPN are hydrogen-rich (CSPN-[O]). Their mass-loss rates lie about one order of magnitude above the dashed $\dot{M}$-L-relation in Fig. 10. Based on the CAK approach to radiation-driven winds, Pauldrach, Hoffmann, and Méndez (2004) managed to calculate hydrodynamically consistent models for such stars (represented by the open circles in Fig. 10), but only when admitting distances, luminosities and masses that seem to be unrealistically large (see the discussion in Sect. 2.3).

Extremely strong is the mass loss from the hydrogen deficient CSPN with Wolf-Rayet type spectra. In analogy to the massive stars, this could be due to a

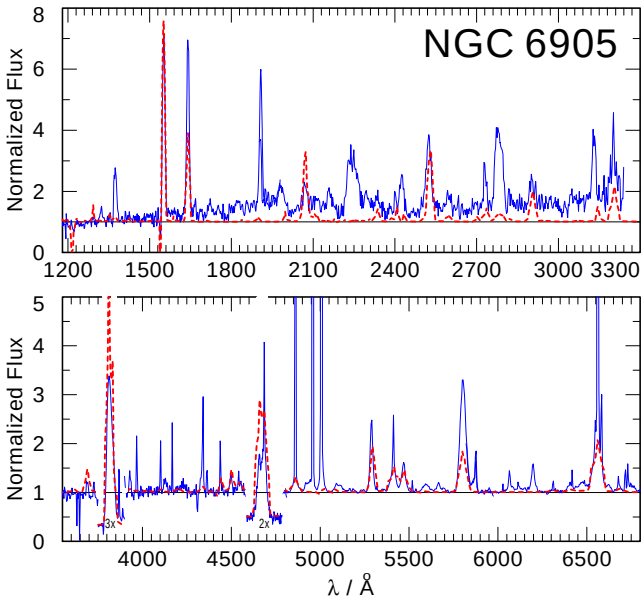

Fig. 11 Observed spectrum of the [WCE]-type central star NGC 6095 (blue line), tentatively fitted with a hydrodynamically consistent model (red-dotted) (from Gräfener, Hamann, and Todt 2008).

closer proximity of the hydrogen-deficient CSPN to the Eddington limit. However, there is no evidence yet that [WC] stars have a higher L/M ratio than central stars of normal surface composition. Nevertheless, Gräfener, Hamann, and Todt (2008) succeeded in calculating a hydrodynamically consistent model for the very hot ($T_* = 200\,\mathrm{kK}$) central star of NGC 6905. Adopting the canonical CSPN luminosity of $5000\,L_\odot$, the model achieved the observed $v_\infty = 2120\,\mathrm{km\,s^{-1}}$. However, the obtained mass-loss rate of $\log \dot{M} = -7.5$ $[M_\odot \mathrm{yr}^{-1}]$ is lower than commonly believed for [WC]-type CSPN, and the agreement with the observed spectrum (see Fig. 11) was achieved by adopting an extremely large clumping contrast of $D = 100$. We argued that the postulated enrichment of the [WC] envelope with s-process elements (which are not included in the wind models) may provide additional radiation driving, but this speculation still needs to be confirmed.

We also studied mass-loss from six extreme helium stars and one sdO, and found that they fall close to or below the dashed $\dot{M}$-L-relation in Fig. 10. Within the group of extreme helium stars, the mass-loss rates scale strongly with the proximity to the Eddington limit. Although the models were not intended to be hydrodynamically consistent, the *a posteriori* comparison between the mechanical energy of the wind and the work done by the radiation pressure revealed in all cases that at least globally the balance is nearly kept. Vice versa, one may consider this agreement as an independent confirmation that the luminosities and distances are correct at least to the order of magnitude.

Acknowledgements

This review is based on collaborative work with Götz Gräfener, Simon Jeffery, Helge Todt, and others.

References

Castor, J.I., Abbott, D.C., Klein, R.I.: Astrophys. J. **195**, 157 (1975)
Georgiev, L.N., Peimbert, M., Hillier, D.J., Richer, M.G., Arrieta, A., Peimbert, A.: Astrophys. J. **681**, 333 (2008)
Gräfener, G., Hamann, W.R.: Astron. Astrophys. **432**, 633 (2005)
Gräfener, G., Hamann, W.R.: Astron. Astrophys. **482**, 945 (2008)
Gräfener, G., Hamann, W., Todt, H.: In: A. Werner & T. Rauch (ed.) Hydrogen-Deficient Stars. Astronomical Society of the Pacific Conference Series vol. 391, p. 99 (2008)
Hamann, W.R., Gräfener, G.: Astron. Astrophys. **427**, 697 (2004)
Hamann, W.R., Feldmeier, A., Oskinova, L.M. (eds.): Clumping in hot-star winds (2008)
Hamann, W., Gräfener, G., Liermann, A.: Astron. Astrophys. **457**, 1015 (2006)
Hamann, W., Gruschinske, J., Kudritzki, R.P., Simon, K.P.: Astron. Astrophys. **104**, 249 (1981)
Heber, U.: Annu. Rev. Astron. Astrophys. **47**, 211 (2009)
Herald, J.E., Bianchi, L.: Astrophys. J. **611**, 294 (2004)
Jeffery, C.S.: Mon. Not. R. Astron. Soc. **235**, 1287 (1988)
Jeffery, C.S., Hamann, W.: Mon. Not. R. Astron. Soc. **in press** (2010)
Krtička, J., Kubát, J.: Astron. Astrophys. **369**, 222 (2001)
Kudritzki, R.P., Urbaneja, M.A., Puls, J.: In: M. J. Barlow & R. H. Méndez (ed.) Planetary Nebulae in our Galaxy and Beyond. IAU Symposium vol. 234, p. 119 (2006)
Marcolino, W.L.F., Hillier, D.J., de Araujo, F.X., Pereira, C.B.: Astrophys. J. **654**, 1068 (2007)
Mereghetti, S., Tiengo, A., Esposito, P., La Palombara, N., Israel, G.L., Stella, L.: Science **325**, 1222 (2009)
Oskinova, L.M., Feldmeier, A., Hamann, W.: Mon. Not. R. Astron. Soc. **372**, 313 (2006)
Oskinova, L.M., Hamann, W., Feldmeier, A.: Astron. Astrophys. **476**, 1331 (2007)
Pauldrach, A.W.A., Hoffmann, T.L., Méndez, R.H.: Astron. Astrophys. **419**, 1111 (2004)
Puls, J., Vink, J.S., Najarro, F.: Astron. Astrophys. Rev. **16**, 209 (2008)
Saio, H., Jeffery, C.S.: Mon. Not. R. Astron. Soc. **333**, 121 (2002)
Schoenberner, D.: Astrophys. J. **272**, 708 (1983)
Schönberner, D., Jacob, R., Steffen, M.: Astron. Astrophys. **441**, 573 (2005)
Springmann, U.W.E., Pauldrach, A.W.A.: Astron. Astrophys. **262**, 515 (1992)
Stasińska, G., Gräfener, G., Peña, M., Hamann, W., Koesterke, L., Szczerba, R.: Astron. Astrophys. **413**, 329 (2004)